Egy. J. Pure & Appl. Sci. 51 (2013) 027-032

Egyptian Journal of Pure and Applied Science

Synthesis and photocatalytic performance of AgO-TiO_2 and AgI-TiO_2 photocatalysts

Heba A. El-Sabban[1, 2*], Mohamed S. Attia[1], Esam Bakir[1] and Mohamed S. A. Abdel-Mottaleb[1]

[1]*Nanophotochemistry and Solar Chemistry Lab, Department of Chemistry, Faculty of Science, Ain Shams University, Abbassia, 11566,Cairo, Egypt,*

[2]*Egyptian Petroleum Research Institute (EPRI), Ministry of Scientific Research, Nasr City, Cairo, Egypt*

ARTICLE INFO

Article history:
Received 22 April 2013
Accepted 27 May 2013

Keywords:
Nanocomposite;
Photocatalyst;
AgO-TiO_2;
AgI-TiO_2;
RBB dye.

ABSTRACT

Nanocomposite photocatalysts AgI-TiO_2 and AgO-TiO_2 were successfully synthesized by thermolysis method at 200°C/2 h. The composite photocatalysts were characterized by XRD, TEM and UV–Vis spectroscopy. The Efficiency of AgI-TiO_2 and AgO-TiO_2 photocatalysts in comparison with pure TiO_2 (P25) was tested by the photocatalytic degradation of Remazol Brilliant Blue RBB dye. The results revealed that the photocatalysts AgI-TiO_2 and AgO-TiO_2 have a higher efficiency than pure TiO_2 (P25) due to increase in surface area of AgO-TiO_2 and AgI-TiO_2 than undoped TiO_2.

Introduction

The removal of dyes from industrial effluents contributes a major problem. Conventional wastewater treatment processes do not remove dyes and colour, as they are fairly stable to light, heat and resist biodegradation because of their complex molecular structures [1]. In recent years several physiochemical decolorisation processes [2] have been developed, such as membrane filtration, flocculation [3], reverse osmosis and biological treatment. In the last few decades, photocatalysts are used for the treatment of environmental pollutants. As one of the most extensively investigated photocatalysts, TiO_2 shows relatively high efficiency, low cost, non-toxicity, and high stability [4–8]. However, TiO_2 can only be activated by ultraviolet (UV) light because it is a large band gap semiconductor (3.2 eV for anatase, 3.0 eV for rutile), and thus only utilizes ~ 5% of the solar spectrum. Moreover, the lack of effective surface area and the high recombination rate of the photogenerated electron-hole pairs in TiO_2 hinders its further application. Therefore, preparation of nanocomposite photocatalysts have been received much attention in the last years. More recently, Li et al. tested the photocatalytic degradation of methyl orange in water and showed that a suitable amount of silver demonstrates a great improvement in the activity compared to pure TiO_2 [9]. Additionally, Hu et al. reported a visible light response AgI-TiO_2 composite photocatalytic material. The catalyst showed high efficiency for the degradation of nonbiodegradable azodyes and maintained high activity in the degradation of K-2G dye (reactive bright red) after six successive cycles under visible light irradiation. Hence, this photocatalyst deserves more attention because of its excellent catalytic activity and reusability [10-11]. Remazol Brilliant Blue (RBB) dye is the commen dye which is used in the dying of textiles. Several methods were used for the getting rid of RBB dye by degradation, such as electrochemical oxidation of aqueous solutions of dye on a boron-doped diamond electrode [12] and also by adsorption onto immobilized Scenedesmus quadricauda [13]. However, these methods are selective, expensive and may need special infrastructure. In this paper, TiO_2 is coupled with semiconductors such as AgI (an ionic semiconductor with direct gap ~2.9 eV) [14] and AgO (a semiconductor with a small indirect gap ~ 0.03eV) [15] by fusion process. The photocalytic efficiency of prepared composites photocatalysts is compared using different molar ratio of dopant and at different temperatures. These prepared composites can compensate for the disadvantages of the separate components such as extending the photon-response range, the efficient separation of the photogenerated electron–hole pairs and the enhancement of the photostability.

Materials and Methods

1. Reagents

All reagents were of pure or analytical grade (Aldrich and Fluka) and were used as received. TiO_2 Degussa

* Corresponding author.
E-mail address: Heba_El-Sabban@hotmail.com

(P25) was used for the preparation of the TiO_2 nanocomposite photocatalysts. The commercially available water-soluble reactive dye Remazol Brilliant Blue (Reactive blue RBB**)** was obtained from Dye Star and used as received. The molecular structure of the dye is given in Fig. 1. The solutions were prepared with pure distilled water.

2. Material synthesis

$AgO-TiO_2$ and $AgI-TiO_2$ nanocomposites were prepared by using silver iodide and silver oxide [15] thermolysis route at 200°C/2 h and 700°C/7 h in the presence of (P-25).

3. Instrumental

3.1. XRD measurements

To determine the crystal phase compositions of the prepared titania nanomaterials, X-ray diffraction measurements were recorded on X'Pert Philips X-ray diffraction (XRD) with Cu-Ka radiation (λ= 1,54056A^0) with accelerating voltage of 40kV and 30mA.

3.2. TEM measurements

Transmission electron microscope, JEM-2000 EX (JEOL, Tokyo, Japan) was used for imaging the prepared nanomaterials. TEM instrument was equipped with Energy dispersive X-ray (EDX, Oxford Instruments INCAx-Sight) for semi-quantitative elemental analysis of the doped titania nanomaterials.

3.3. Surface area measurements

The specific surface area was calculated by the BET equation. The pore size distribution was determined by adsorption branch.

3.4. Photoillumination setup: A home-made photo reactor (PHOCAT 120)

PHOCAT 120 is designed for Top and Side irradiation. Different wavelength ranges in UV and visible spectrum regions are provided by black, blue or white broadband fluorescent lamps (88 Watts).The chamber is provided with water-cooled capability. The efficient airflow design stabilizes the temperature about 3 degrees Celsius above room temperature.

Results and discussion

1. Catalyst characterization

1.1. XRD spectra

The XRD peaks of pure TiO_2 at 2θ = 25.12, 37.76, 54.08, 62.56, 75.12 are easily identified as TiO_2 in the anatase form, a weak peak at 2θ = 27.2 represent the rutile form, see Fig.2. The XRD patterns are clearly showing a new characteristic peak at 2θ = 36.8 indicating the presence of AgO as shown in Fig.3 and a new characteristic peak at 2θ =23.66, 56.48 for AgI, Fig.4.

The average crystalline diameters were calculated from scherrer's equation and decreases in the order $AgO-TiO_2$ at 700°C (54.9 nm) > TiO_2 (33.8 nm) > $AgI-TiO_2$ at 200°C (32.7 nm) > $AgO-TiO_2$ at 200°C (30.9 nm) as shown in Table 1. XRD patterns of $AgO-TiO_2$ at 700°C shows increase in particle size and very weak peak for anatase form, Fig.5.

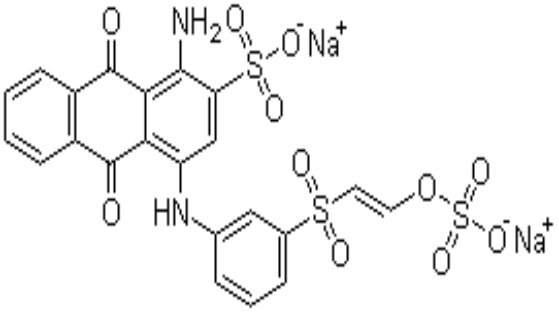

Fig. 1: Remazol Brilliant Blue R; 2-(3-(4-Amino-9, 10-dihydro-3-sulpho-9, 10-dioxoanthracen- 4-yl) aminobenzenesulphonyl) vinyl) disodium sulphate. Molecular Formula $C_{22}H_{16}N_2Na_2O_{11}S_3$ (M.wt = 626.54).

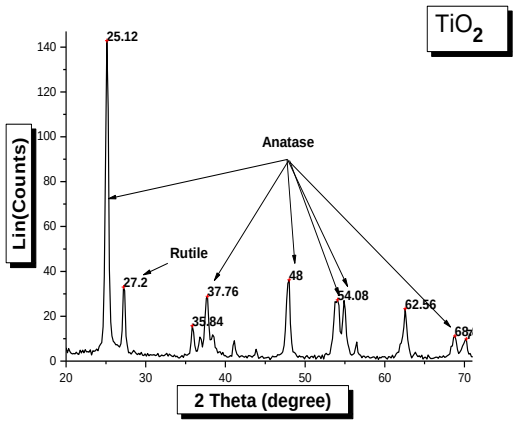

Fig. 2: XRD pattern of pure TiO_2.

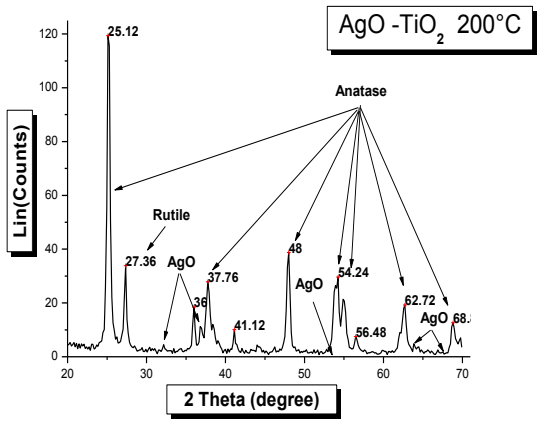

Fig. 3: XRD pattern of $AgO-TiO_2$ sample prepared at 200°C/2 h.

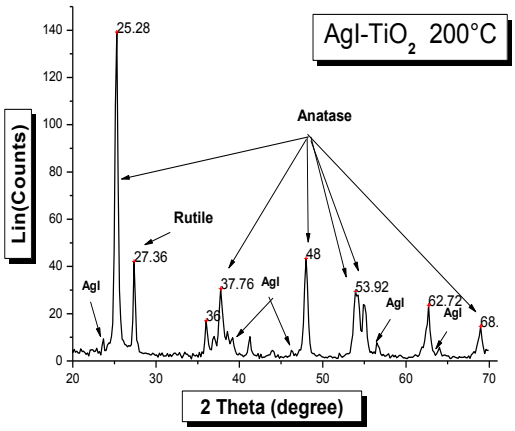

Fig. 4: XRD pattern of $AgI-TiO_2$ sample prepared at 200°C/ 2 h.

Table 1: Crystal parameters data of pure TiO_2, AgO-TiO_2 and AgI-TiO_2 prepared at different temperatures.

Samples	Phase	X%	L(nm)
TiO_2	Anatase Rutile	77.25 % 22.75 %	33.8
AgI-TiO_2 200°C	Anatase Rutile	72.17 % 27.83 %	32.7
AgO-TiO_2 200°C	Anatase Rutile	73.51 % 26.49 %	30.9
AgO-TiO_2 700°C	Anatase Rutile	26.74 % 73.26 %	54.9

1.2. TEM images

Fig. 6 (a-d) shows TEM images of nanocatalysts. The particle size of doped TiO_2 nanocatalysts decrease in the same order AgO-TiO_2 at 700°C (81.17 nm) > TiO_2 (33.5 nm) > AgI-TiO_2 at 200°C (21.3 nm) > AgO-TiO_2 at 200°C (13.12 nm).

1.3. BET analysis

The specific surface area (S_{BET}), total pore volume (V_p) and average pore diameter of the nanocomposite photocatalysts were measured by the BET method and the results are also listed in Table 2.

2. Photodegradation experiments

The change in the absorption spectra of aqueous solutions of Remazol Brilliant Blue RBB dye as a function of UV–Vis irradiation has been monitored with initial $4.2X10^{-5}$ M dye concentration and 1.0 g L^{-1} of undoped and doped TiO_2 catalyst at its neutral pH value. As seen in Fig. 7 (a-b), the reductions in the main characteristic absorbance peak of the dye in the presence of 0.4% AgI-TiO_2 and 0.6% AgO-TiO_2 at 200°C indicate the decolorization of the dye.

To evaluate the effects of AgI and AgO concentrations on the photocatalytic activity of TiO_2, we carried out set tests to decolorize RBB dye in aqueous suspensions with an initial concentration of $4.2X10^{-5}$ M under UV–Vis illumination by using TiO_2 nanoparticles with different dopant concentrations.

The decolorization rate kinetics of RBB is found to obey first order rate kinetics confirmed by the linear fit equation

$$ln\ A_t = ln\ A_0 - kt \quad (1)$$

where k is the rate constant (min^{-1}), t is the irradiation time, A_0 and A_t are the initial and final absorption values of the dye solution, respectively. A plot of $ln(A_t/A_0)$ versus t yields a straight line. The photocatalytic initial decolorization rates of Remazol RBB using TiO_2 nanoparticles with different dopant concentrations calcined at 200°C are shown in Fig.8 (a-b). By increasing the temperature of calcinations up to 700°C, the reduction in the phtocataltic activity was obtained compared to other composite photocatalysts, Fig.8 (c). Results are summarized in Table 3.

The experiment demonstrated that all AgI-TiO_2 and AgO-TiO_2 catalysts achieved higher rates of RBB degradation than the pure TiO_2 catalyst. The enhancement of RBB degradation rate increased with the increase of AgI and AgO content initially, but declined while the AgI and AgO content reached a higher level. The results indicated that 4% AgI-TiO_2 and 6% AgO-TiO_2 achieved the best performance under UV–Vis illumination, the insets in Fig.8 and Table 3.

3. The mechanism of Remazol blue RBB degradation enhancement by using AgI-TiO_2 and AgO-TiO_2 photocatalysts

The efficiency of Remazol Brilliant Blue RBB photocatalytic degradation strongly depends on the photocatalytic activity of nanocomposite photocatalysts, which are affected by their band gap and surface properties. In our investigation, 4% AgI-TiO_2 and 6% AgO-TiO_2 catalysts prepared at 200°C shows more photocatalytic efficiency than pure TiO_2. Increasing the molar ratio of AgI and AgO in doped titanium above the optimum ratio may leads to the poisoning of the active sites of TiO_2 thus limits its photocatalytic activity.

The improvement of photocatalytic activity of TiO_2 is due to narrowing the band gap of TiO_2 by doping it with narrow band gap semiconductors such as AgI (~2.9 eV) and AgO (0.03eV). Doping of TiO_2 with AgI and AgO is

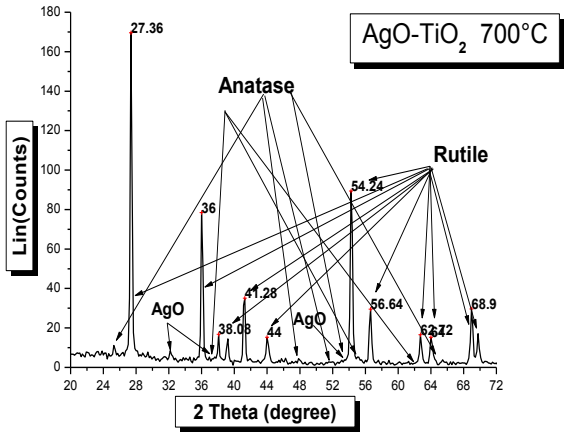

Fig. 5: XRD image of AgO-TiO_2 sample prepared at 700°C/7 h.

expected to extend its photoresponse towards the visible regions of the spectrum with the additional advantage that the co-doping of AgI and AgO suppresses the undesired recombination of photo-generated electrons with the holes (e^-/h^+ recombination).

The higher photocatalytic efficiency of AgO-TiO_2 than AgI-TiO_2 is attributed to the fact that the energy gap of AgO (0.03eV) is smaller than that of AgI (~2.9 eV). This leads to narrowing the band gap of TiO_2 when doping with AgO than when doping with AgI extending the photoresponse of AgO-TiO_2 towards the visible regions.

XRD patterns and TEM photographs show decrease in particle size of doped TiO_2 calcined at 200°C enhancing its photocatalytic efficiency than pure TiO_2. AgO-TiO_2 shows highest photocatalytic activity due to increase in its surface area in comparison with other composites.

According to N_2 adsorption–desorption isotherms and pore size distribution, the 6% AgO-TiO_2 catalyst has the highest surface area. This result illustrates the best performance for RBB removal using 6% AgO-TiO_2 photocatalyst in comparison with the other catalysts as shown in Table 2.

Alternatively, the modification of the surface state and valence band structure of the catalysts might be another critical reason for promoting the photocatalytic activity.

Conclusion

The prepared AgI-TiO_2 and AgO-TiO_2 calcined at 200°C display enhanced visible light absorption, and the photocatalytic activity against RBB dye is greatly improved in comparison with pure TiO_2. The enhancement in the visible light photocatalytic performance of the AgI-TiO_2 and AgO-TiO_2 could be attributed to AgI and AgO with narrow band gap, increase in surface area of doped TiO_2 and the effective electron–hole separations at the interfaces of the two semiconductors, which facilitate the transfer of the photoinduced carriers. AgO-TiO_2 shows more efficient photocatalytic efficiency than AgI-TiO_2 as it reveals decrease in particle size and increase in surface area.

By increasing the temperature of calcination up to 700°C, AgO-TiO_2 shows obvious increase in particle size and disappearance of anatase form that considered being more active than rutile form thus limiting its photocatalytic efficiency.

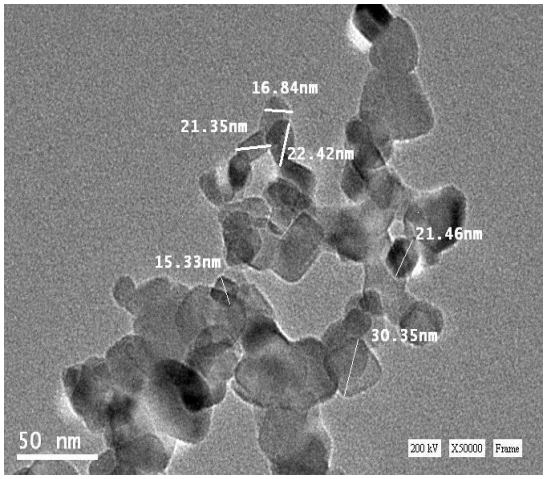

Fig. 6a: TEM image of AgI-TiO_2 sample prepared at 200° C /2 h.

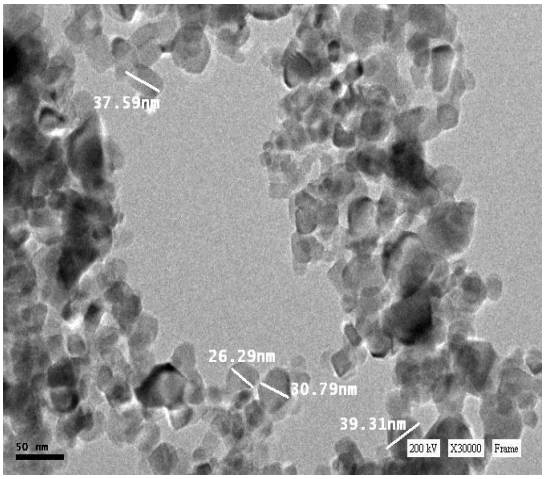

Fig. 6c: TEM image of pure TiO_2 sample.

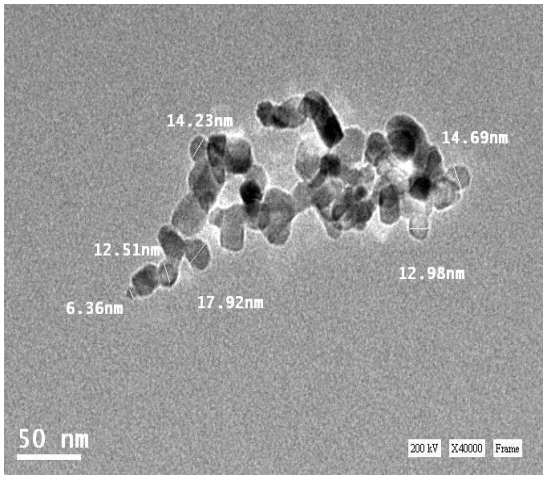

Fig. 6b: TEM image of AgO-TiO_2 sample fused at 200° C /2 h.

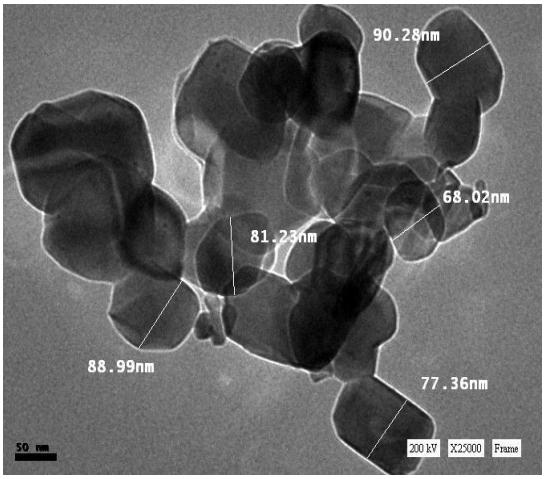

Fig. 6d: TEM image of AgO-TiO_2 sample prepared at 700°C /2 h.

Table 2: Surface area, total pore volume and average for various solid samples.

Samples	Surface area (m^2/g)	Total pore volume	Average pore size
TiO_2	40.66	0.0199	19.67
AgI-TiO_2 200°C	57.9	0.026	17.94
AgO-TiO_2 200°C	71.15	0.03	16.98
AgO-TiO_2 700°C	11.69	0.005	17.41

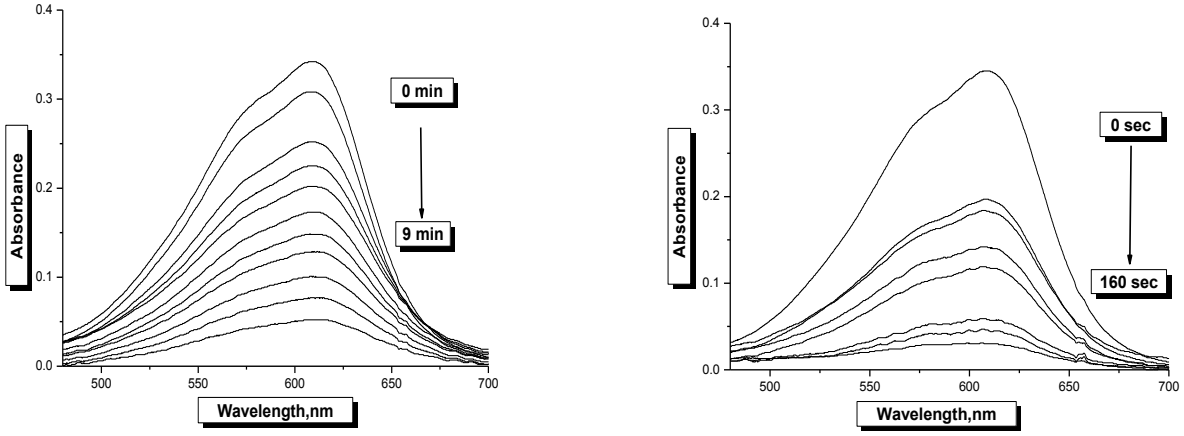

Fig.7: Photodegradation of 4.2X10^{-5} M RRB using TiO_2 doped with (a) AgI (4%) and (b) AgO (6%) at 200° C /2 h.

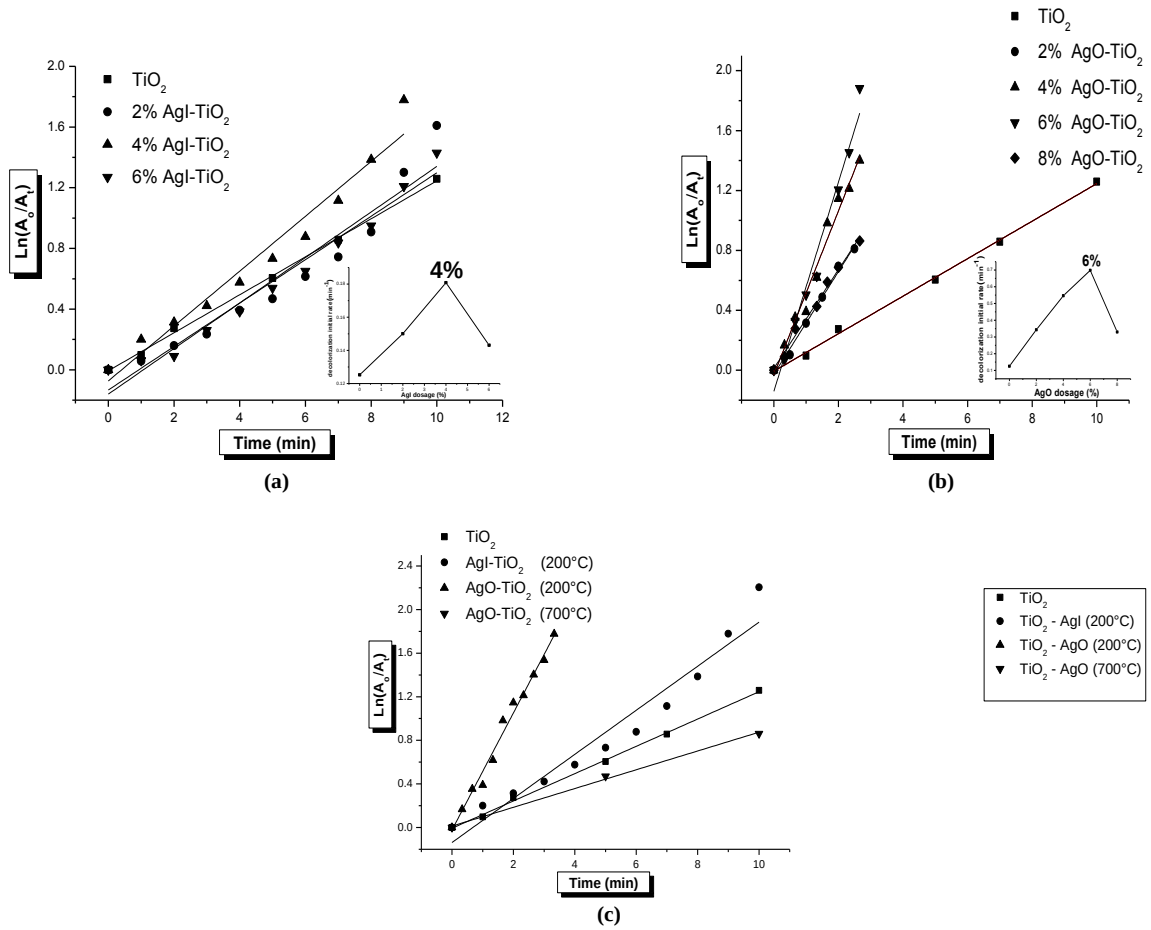

Fig.8: The photocatalytic properties of titania-doped different contents of (a) AgI and (b) AgO at 200°C for 2 h in air on RBB (4.2X10^{-5} M). Insets: The photoreaction kinetic constant (k_r) vs. AgI and AgO dosage.

Table 3: The conventional parameter characterization of photooxidation of Remazol Brilliant Blue RBB using undoped and doped TiO_2.

Catalyst	**k(min^{-1})x10^3**
TiO_2 200°C/2 h	125.24
2% AgI-TiO_2 200°C/2 h	150.07
4% AgI-TiO_2 200°C/2 h	180.84
6% AgI-TiO_2 200°C/2 h	143.16
2% AgO-TiO_2 200°C/2 h	342.68
4% AgO-TiO_2 200°C/2 h	546.57
6% AgO-TiO_2 200°C/2 h	698.51
8% AgO-TiO_2 200°C/2 h	329.59
4% AgO-TiO_2 700°C/2 h	86.13

References

1) **Rashmi, S. and Bani, B. (2003).** Adsorption-coagulation for the decolorisation of textile dye solutions. Water Qual. Res. J. Canada 38: 553-562.
2) **Reife, A. (1993).** Kirk Othmer encyclopedia of chemical technology and encyclopedia of environmental remediation. John Wiley and Sons, N.Y. p. 753-783.
3) **Stephenson, R.J. and Sheldon, J.B. (1996).** Coagulation and precipitation of a mechanical pulping effluent. Water Res. 30:781–792.
4) **Zang, Y. and Farnood, R., (2004).** Photocatalytic decomposition of methyl tert-butyl ether in aqueous slurry of titanium dioxide. Appl. Catal. B 57: 273-279.
5) **Yu, J.C., Ho, W., Yu, J., Yip, H., Wong, P.K. and Zhao, J. (2005).** Efficient visible-light-induced photocatalytic disinfection on sulfur-doped nanocrystalline titania. Environ. Sci. Technol. 39: 1175-1179.
6) **Wolfrum, E.J., Huang, J., Blake, D.M., Maness, P.C., Huang, Z., Fiest, J. and Jacoby, W.A. (2002).** Photocatalytic oxidation of bacteria, bacterial and fungal spores, and model biofilm components to carbon dioxide on titanium dioxide-coated surfaces. Environ. Sci. Technol. 36: 3412-3419.
7) **Mill, A. and Hunte, S.L. (1997).** An overview of semiconductor photocatalysis. Photochem. Photobiol. A: Chem. 108: 1-35.
8) **Zhao, W., Wang, X., Sang, H. and Wang, K. (2013).** Synthesis of Bi-doped TiO_2 nanotubes and enhanced photocatalytic activity for hydrogen evolution from glycerol solution. Chinese J Chem. 31: 415-420.
9) **Li, H., Duan, X., Liu, G. and Liu, X. (2008).** Photochemical synthesis and characterization of Ag/TiO_2 nanotube composites. Mater. Sci. 43: 1669-1676.
10) **Hu, C., Hu, X., Wang, L., Qu, J. and Wang, A. (2006).** Visible-light-induced photocatalytic degradation of azodyes in aqueous AgI/TiO_2 dispersion. Environ. Sci. Technol. 40: 7903-7907.
11) **Hu, C., Guo, J., Qu, J. and Hu, X. (2007).** Photocatalytic degradation of pathogenic bacteria with AgI/TiO_2 under visible light irradiation. Langmuir 23: 4982-4987.
12) **Montanaro, D. and Petrucci, E. (2009).** Electrochemical treatment of Remazol Brilliant Blueon a boron-doped diamond electrode. Chem. Eng. 153: 138-144.
13) **Ergene, A., Ada, K., Tan, S. and Katırcıoğlu, H. (2009).** Removal of Remazol Brilliant Blue R dye from aqueous solutions by adsorption onto immobilized Scenedesmus quadricauda: Equilibrium and kinetic modeling studies. Desal. 249: 1308-1314.
14) **Freedhoff, M.I., Marchettib, A.P. and McLendond, G.L., (1996).** Optical properties of nanocrystalline silver halides. Lumin. 70: 400-413.
15) **Park, K.-T., Novikov, D.L., Gubanov, V.A. and Freeman, A.J. (1994).** Electronic structure of noble-metal monoxides: PdO, PtO and AgO. Phys. Rev. B 49: 4425-4431.